Journal of Peptide Science
J. Peptide Sci. 2006; **12**: 443–454
Published online 23 January 2006 in Wiley InterScience (www.interscience.wiley.com). DOI: 10.1002/psc.747

JOURNAL OF PEPTIDE SCIENCE

Orexin-A is composed of a highly conserved *C*-terminal and a specific, hydrophilic *N*-terminal region, revealing the structural basis of specific recognition by the orexin-1 receptor

TOMOYO TAKAI,[a] TAKAO TAKAYA,[b] MUTSUKO NAKANO,[b] HIDEO AKUTSU,[a] ATSUSHI NAKAGAWA,[a] SABURO AIMOTO,[a] KATSUYA NAGAI[a] and TAKAHISA IKEGAMI[a]*

[a] Institute for Protein Research, Osaka University, Yamadaoka 3-2, Osaka, 565-0871, Japan
[b] Osaka Technology Licensing Organization, Business Innovation Center Osaka 14F, 1-4-5 Hommachi, Chuo-ku, Osaka-shi, 541-0053, Japan

Received 27 September 2005; *Revised 30 November 2005*; *Accepted 30 November 2005*

Abstract: Orexins-A and B, also called hypocretins-1 and 2, respectively, are neuropeptides that regulate feeding and sleep-wakefulness by binding to two orphan G protein-coupled receptors named orexin-1 (OX_1R) and orexin-2 (OX_2R). The sequences and functions of orexins-A and B are similar to each other, but the high sequence homology (68%) is limited in their *C*-terminal half regions (residues 15–33). The sequence of the *N*-terminal half region of orexin-A (residues 1–14), containing two disulfide bonds, is very different from that of orexin-B. The structure of orexin-A was determined using two-dimensional homonuclear and ^{15}N and ^{13}C natural abundance heteronuclear NMR experiments. Orexin-A had a compact conformation in the *N*-terminal half region, which contained a short helix (III : Cys6-Gln9) and was fixed by the two disulfide bonds, and a helix-turn-helix conformation (I : Leu16-Ala23 and II : Asn25-Thr32) in the remaining *C*-terminal half region. The *C*-terminal half region had both hydrophobic and hydrophilic residues, which existed on separate surfaces to provide an amphipathic character in helices I and II. The nine residues on the hydrophobic surface are also well conserved in orexin-B, and it was reported that the substitution of each of them with alanine resulted in a significant drop in the functional potency at the receptors. Therefore, we suggest that they form the surface responsible for the main hydrophobic interaction with the receptors. On the other hand, the residues on the hydrophilic surface, together with the hydrophilic residues in the *N*-terminal half region that form a cluster, are known to make only small contributions to the binding to the receptors through similar alanine-scan experiments. However, since our structure of orexin-A showed that large conformational and electrostatical differences between orexins-A and B were rather concentrated in the *N*-terminal half regions, we suggest that the region of orexin-A is important for the preference for orexin-A of OX_1R.

Keywords: orexin; GPCR; narcolepsy; feeding; protein structure

INTRODUCTION

Orexin-A and orexin-B [1], also called hypocretin-1 and hypocretin-2 [2], respectively, are neuropeptides, which are generated through the proteolytic cleavage of a common precursor, prepro-orexin or prepro-hypocretin, composed of 131 amino acid residues. Orexins-A and -B bind to two mutually, closely related (64% homology) orphan G protein-coupled receptors (GPCRs), named orexin-1 (OX_1R) and orexin-2 (OX_2R) receptors to activate them [1]. The messenger-RNA of the precursor is specifically expressed in the lateral hypothalamus area (LHA), known as a feeding center. Since intracerebroventricular administration of orexins stimulates feeding in rats and mice, and orexins are colocalized with other orexigenic peptides including dynorphin and galanin, orexins are thought to function as potent orexigenic peptides (the Greek word 'orexis' meaning appetite). Furthermore, orexin-knockout mice exhibit a syndrome similar to human narcolepsy [3]. Therefore, it is suggested that orexins play an important role in regulating feeding and sleep-wakefulness by modulating energy metabolism [4–6]. It has also been reported that orexin-A affected stimulation of feeding behavior and food intake to a more potent degree and for a longer period than orexin-B [1,7,8], and that the treatment of rat LHA with another feeding-related peptide, leptin, led to a significant decrease in the orexin-A concentration [9] as well as to a decrease in the messenger-RNA level of OX_1R, which binds more selectively to orexin-A [10]. Thus, orexin-A is more involved, particularly in regulating feeding.

The sequence of orexin-A (the molecular weight, 3561.1) is pyroglutamic (Pyr)-PLPDCCRQKTCSCRLYE-LLHGAGNHAAGILTL-NH_2, where the *N*- and *C*-termini are modified with Pyr acid and an amino group,

Abbreviations: COSY, correlated spectroscopy; GPCR, G protein-coupled receptors, HSQC, heteronuclear single quantum correlation; NMR, nuclear magnetic resonance; NOE, nuclear *Overhauser* effect; NOESY, NOE spectroscopy; RMSD, root mean square deviation; TOCSY, total correlation spectroscopy.

*Correspondence to: T. Ikegami, Institute for Protein Research, Osaka University, Yamadaoka 3-2, Osaka, 565-0871, Japan;
e-mail: tiik@protein.osaka-u.ac.jp

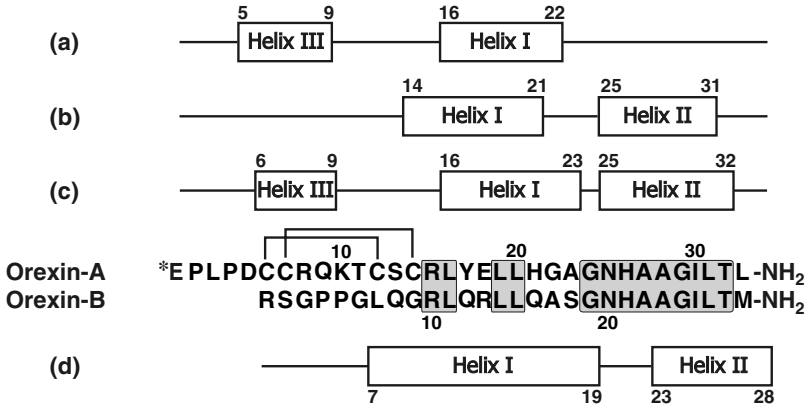

Figure 1 The amino acid sequences of orexins-A and -B, and their secondary structures. The one-letter code of the first *N*-terminal residue of orexin-A (*E) represents pyroglutamic acid. The *C*-termini of both orexins ($-NH_2$) are amidated. Two intramolecular disulfide bonds in orexin-A formed between Cys6 and Cys12, and between Cys7 and Cys14 are shown as lines. The residues, identical in both orexins, are boxed in shading. The secondary structures described in the literature are indicated by boxes with the starting and ending sequence numbers: (a) orexin-A in (SDS)-micelles by Miskolzie *et al.* [11], (b) orexin-A by Kim *et al.* [12], (c) our orexin-A structure, and (d) orexin-B by Lee *et al.* [13].

respectively (Figure 1). Two intramolecular disulfide bonds are formed between Cys6 and Cys12, and between Cys7 and Cys14. Orexin-B has no Pyr acid in its *N*-terminus, but the *C*-terminus is amidated through a posttranslational modification as that for orexin-A. The sequences of orexin-A are completely conserved among several vertebrates, and those of orexin-B are also highly (93%) conserved among species with two residues substituted in rat and mouse (Pro2 and Asn18) compared to those in humans (Ser2 and Ser18). Human orexin-B, constituted of 28 amino acid residues, has 46% sequence homology to human orexin-A, which is constituted of 33 residues, but the similarity is limited to the *C*-terminal half region following Arg15 in orexin-A (Arg10 in orexin-B) (Figure 1). The *N*-terminal region in orexin-A (Pyr1 to Cys14) containing the two disulfide bonds exhibits only 11% similarity to the corresponding part of orexin-B (Arg1 to Gly9), as can easily be expected from the lack of a disulfide bond in orexin-B, while the remaining *C*-terminal parts of orexins-A and -B share 68% homology. The comparison between the sequences led to a prediction that the three-dimensional structures of orexins-A and -B would also be similar in their *C*-terminal regions but different in their *N*-terminal regions.

The solution structure of human orexin-B was recently determined by two-dimensional (2D) ^{1}H nuclear magnetic resonance (NMR) spectroscopy [13], and then the structures of orexins-A and -B bound to deuterated sodium dodecylsulfate (SDS) micelles were also determined by 2D ^{1}H and the natural abundance ^{13}C NMR spectroscopy [11]. The structure of orexin-B dissolved in H_2O (pH 3.5) consists of two α-helices (helix I : Leu7-Gly19 and helix II : Ala23-Met28) making various angles within 60–80° relative to each other, and a flexible linker connecting these helices (Figure 1(d) and 5). Orexin-A in SDS micelles tends to adopt a conformation containing an α-helix composed of seven residues (helix I : Leu16-Gly22), which, however, corresponds only to the *C*-terminal part of helix I in orexin-B (Leu11-Ala17) (Figure 1(a) and (d)). The region in orexin-A (Cys12-Arg15) that corresponds to the remaining *N*-terminal part of helix I in orexin-B (Leu7-Arg10) had no helical conformation, perhaps owing to a steric hindrance caused by the two disulfide bonds formed in this region of orexin-A. Although the conformations in helix I of orexin-A in micelles were well converged in the NMR ensemble structures, the orientations of the remaining *N*- and *C*-terminal regions with respect to helix I were dispersed [11]. Furthermore, the conformation in the *C*-terminal region following helix I was unknown as seen in the results of Miskolzie *et al.* [11]. Voisin *et al.* [14] predicted, by homology modeling using software Modeller-6.0, that orexin-A had a conformation almost the same as that of orexin-B on the basis of the high sequence homology between them. However, this prediction needs to be confirmed by experimental observation, in particular, for the conformation in the region containing the two disulfide bonds in orexin-A, ranging from Cys6 to Cys14, since this region has a low sequence homology (11%) to orexin-B, which has no disulfide bond. Here, we report the refined structure of orexin-A dissolved in water, which has allowed us to further discuss the interaction with the receptors using the accumulated biological data, including mutational works. Very recently, Kim *et al.* [12] presented the solution structure of human orexin-A. Their structures contain two α-helices, for which the ranges and relative bending degree were similar to those of our structures (Figure 1(b) and (c)). However, for the above-mentioned *N*-terminal part, we have determined significantly different conformations from theirs and also from the structures of orexin-B. It is thought that the *N*-terminal part of orexin-A plays an especially important role in

being distinct from orexin-B. Using both structures as well as the conformation of orexin-A in micelles [11], we discuss the characters separated in the *N*- and *C*-terminal regions, which must be important in binding to the receptors, and propose a possible conformational exchange in the *N*-terminal region in solution that may have a biological significance in binding to the membranes and receptors.

MATERIALS AND METHODS

Sample Preparation

The human orexin-A sample, chemically synthesized and purified with a reversed-phase column (YMC Pack ODS A-302), was purchased from Peptide Institute, Inc. (Osaka, Japan). The solvent was exchanged with an 18 mM potassium phosphate buffer (pH 6.0) containing 10% D_2O using the ultrafiltration method (Microsep™ Centrifugal Devices with the molecular cut of 1000), and the contaminated impurities such as acetonitrile were washed out at the same time by repeating the filtration five times. The proteins were concentrated to 0.76 mM, which was estimated by absorbance at 280 nm using the calculated molar absorption coefficient at 280 nm of 1520 $m^{-1}cm^{-1}$. The protein dissolved in D_2O was made by lyophilizing a concentrated sample that contained the same H_2O-based buffer and then dissolving it with the same amount of 99.9% D_2O. The solution of 260 µl was sealed in a Shigemi NMR micro tube of 5 mm diameter (BMS-3) for the NMR measurements.

NMR Spectroscopy

Most NMR experiments were performed with a Bruker DRX600 spectrometer equipped with a triple resonance probe with a self-shielded triple axis gradient coil, or DRX800 with a cryogenic probe at 293 K. The following spectra were acquired for the resonance assignments: 2D-DQF-COSY, TOCSY with the mixing time of 69 ms, NOESY with the mixing times of 100 and 150 ms, $^{15}N-^{1}H$-heteronuclear single quantum correlation (HSQC), and $^{13}C-^{1}H$-HSQC, both measured by the gradient-echo method at natural abundance. The NOESY and TOCSY spectra were measured for both samples dissolved in H_2O and D_2O. The number of complex points and spectral widths for each experiment were as follows: DQF-COSY (5120, 12 019 Hz (F_2) * 900, 5319 Hz (F_1), at the 600 MHz ^{1}H resonance frequency, with 32 scans), TOCSY (5120, 12 019 Hz (F_2) * 750, 5319 Hz (F_1), at the 600 MHz, with 16 scans), NOESY (5120, 12 821 Hz (F_2) * 800, 7463 Hz (F_1), at the 800 MHz, with 64 scans), $^{15}N-^{1}H$-HSQC (1024, 12 820 Hz (F_2) * 128, 2778 Hz (F_1), at the 800 MHz, with 256 scans), and $^{13}C-^{1}H$-HSQC (1024, 14 368 Hz (F_2) * 400, 15 625 Hz (F_1), at the 800 MHz, with 64 scans). Amide proton exchange with the solvent deuteron was observed in a 2D-TOCSY experiment with the mixing time of 40 ms. The measurement was continued for 6 h on DRX500 at 293 K after dissolving lyophilized and protonated orexin-A with the same buffer content into 99.9% D_2O. The resonances observed in the spectrum were identified as being derived from the amide protons involved in hydrogen bonding. In the measurements with the samples dissolved in H_2O, a large water signal was suppressed by the WATERGATE method, and the indirect dimensions (F_1) were acquired by the States-TPPI manner for the 2D-homonuclear experiments and by the gradient-echo (sensitivity enhancement) manner for both ^{13}C and ^{15}N HSQC experiments [15]. The NMR data were processed and analyzed using the nmrPipe [16] and Sparky (developed by T. D. Goddard and D. G. Kneller in UCSF) software packages, respectively.

Structure Calculation

The nuclear *Overhauser* effect (NOE) connectivities derived from strong, medium, and weak cross peaks were categorized and assumed to correspond to the upper limits for the interproton distance restraints of 3.0, 4.0, and 5.0 Å, respectively. Pseudo-atom corrections were applied to the upper bound restraints involving methyl, methylene, and aromatic ring protons as described [17]. The distance restraints for the hydrogen bonds, applied for slowly exchanging amides after the root mean square deviation (RMSD) value for the overlaid backbone atoms of calculated structures reached 1.5 Å, were 2.8–3.3 Å for N–O pairs and 1.8–2.3 Å for H–O pairs. The acceptors of the hydrogen bonds in α-helices were determined on the basis of the backbone torsion angle information and the short and medium range NOE patterns, $d_{\alpha N(i,i+3)}$ and $d_{\alpha N(i,i+4)}$, where the notation $d_{\alpha N(i,j)}$, e.g. represents the connectivity between the α proton resonance of the ith amino acid and the amide proton resonance of the jth amino acid in the sequence. The restraints for the two disulfide bonds were included after the backbone RMSD reached 1.5 Å, according to the CYANA standard procedure [18], where three restraints were applied per disulfide bridge between the residue numbers i and j in the form of $2.0 \leq d(S_i^{\gamma}, S_j^{\gamma}) \leq 2.1$ Å, $3.0 \leq d(C_i^{\beta}, S_j^{\gamma}) \leq 3.1$ Å, and $3.0 \leq d(S_i^{\gamma}, C_j^{\beta}) \leq 3.1$ Å. The backbone torsion angles were predicted using TALOS software [19] with the assigned chemical shifts of $^{13}C_{\alpha}$, $^{13}C_{\beta}$, $^{1}H_{\alpha}$, and ^{15}N, which were calibrated with 2,2-dimethyl-2-silapentane-5-sulfonate sodium salt (DSS). The restraints for the backbone dihedral angles, ϕ and ψ, were applied in the form of the average $\pm$ once or twice the standard deviation, as long as TALOS categorized the corresponding angles as 'Good' or 'New', respectively. The structures were calculated with CYANA-2.0 software [18] by molecular dynamics in a torsion angle space with 4000 steps. After well-converged structures with the RMSD of <1.0 Å for the backbone atoms were obtained, the pseudo-atom corrections for the center averaging were removed, and instead the r^{-6} sum averaging method for the degenerate protons in the methyl and aromatic protons and the floating chirality approach for the diastereotopic groups such as methylene protons were applied as the default in the CYANA calculations [18]. The 30 structures with the lowest target functions among the 100 calculated ones were analyzed with MOLMOL [20] and with AQUA-PROCHECK-NMR [21] software. The secondary structures were determined on the basis of the main-chain hydrogen bond patterns, NOE connectivities, and the results of the AQUA-PROCHECK-NMR analysis [21].

RESULTS

Chemical Shift Assignments and the Secondary Structures

The human orexin-A was chemically synthesized in the nonlabeled form, and purified with HPLC for NMR

studies. To assign the resonance signals of orexin-A, the standard methods of NMR for nonlabeled proteins were used. The structures of orexin-A were determined using 2D homonuclear and ^{15}N and ^{13}C natural abundance heteronuclear NMR experiments. The 2D $^{1}H-^{15}N$ HSQC experiment exhibited well-dispersed ^{1}H and ^{15}N resonances of the main-chain amide protons (Figure 2). The combination of $d_{\alpha N(i,i+1)}$ NOE connectivities in the 2D NOESY spectra and $d_{\alpha N(i,i)}$ scalar coupled connectivities in 2D TOCSY and DQF-COSY spectra allowed for sequential resonance assignments of the backbone. The amino acid spin systems were identified on 2D TOCSY and DQF-COSY spectra. The assigned chemical shifts of orexin-A have been registered at BioMagResBank (http://www.bmrb.wisc.edu/index.html) with the accession code of 6441. The short and medium range upper distance limits applied are plotted against the amino acid sequence in Figure 3(a). NOE cross peaks characteristic of α-helix, $d_{NN(i,i+1)}$, $d_{\alpha N(i,i+3)}$, and $d_{\alpha\beta(i,i+3)}$, were observed in Asp5-Lys10, Cys14-Gly22, and Asn25-Ile30. However, because the chemical shifts of the amide protons of Ala27, Ala28, and Gly29 overlapped, $d_{NN(i,i+1)}$ cross peaks for these residues failed to be identified. Furthermore, some other peak overlaps in the Hα resonance region of Ala28-Leu33 hindered the NOE assignments. The peptide bonds of both Pro2 and Pro4 were determined to take a *trans* conformation on the basis of the NOEs observed between the δ-protons of the prolines and the α-protons of the preceding residues.

Structure Calculation

The three-dimensional structures of human orexin-A (PDB code: 1WSO) were calculated by the software CYANA [18] using the experimental restraints composed of 373 interproton distance restraints derived from NOE, 48 dihedral angle restraints basically estimated from deviations of the related chemical shifts from those of random coils, 9 hydrogen bond restraints involving amide protons that exchanged slowly with solvent deuterons, and 2 disulfide bridge restraints. The 30 best structures with the lowest target functions, 0.14 ± 0.03 Å on average, among 100 calculated ones showed no distance restraint violation of >0.2 Å and no dihedral angle restraint violation of $>5^{\circ}$. Superposition of these 30 structures is displayed in Figure 4(a), and the restraints applied and the structural statistics for the final structures are listed in Table 1. The RMSD of these structures to the mean were 0.91 Å (Pyr1-Ala23) (Figure 4(b)) and 0.34 Å (Asn25-Leu33) (Figure 4(c)) for the backbone heavy atoms, and 1.64 Å (Pyr1-Ala23) and 1.33 Å (Asn25-Leu33) for all the heavy atoms. All the ϕ and ψ dihedral angles, except for those of the *C*-terminal Leu33 for the final 30 structures, were distributed within the allowed regions in the Ramachandran plot (Figure 3(b)). The secondary structures of human orexin-A were defined as Cys6-Gln9 (helix III), Leu16-Ala23 (helix I), and Asn25-Thr32 (helix II) (Figure 1(c)). Helices I and II were connected by a flexible residue, Gly24. As displayed in the Ramachandran plot in Figure 3(b), the ϕ and ψ dihedral

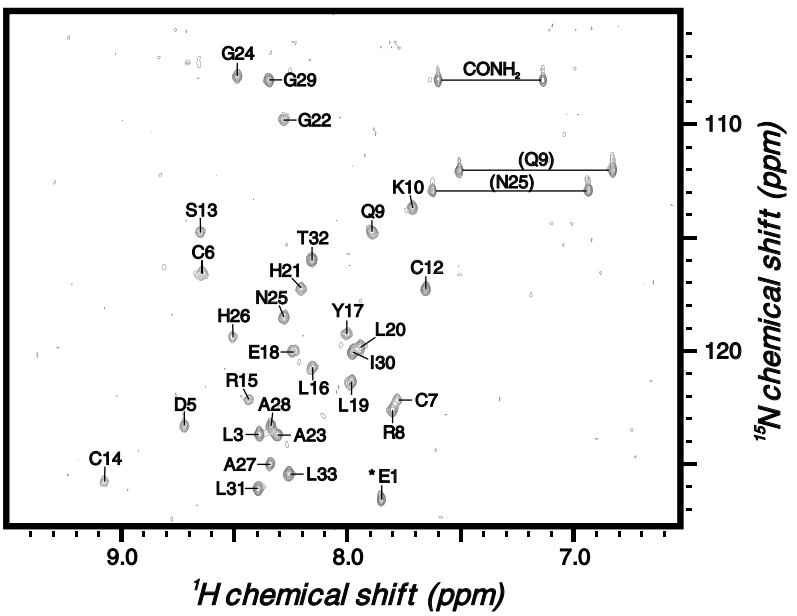

Figure 2 A $^{15}N-^{1}H$-HSQC spectrum of orexin-A. The spectrum of orexin-A (0.76 mM) was obtained by the gradient-echo method [15] at the natural abundance of ^{15}N nuclei on a DRX800 spectrometer with a cryogenic probe at 293 K. The ^{1}H and ^{15}N chemical shift evolutions were sampled at 1024 and 128 complex points, respectively, with 256 scans accumulated for each free induction decay (FID). The measurement time took 42 h in total. The assignment of each peak to the corresponding amide $^{1}H-^{15}N$ group is indicated. The amide group in the first pyroglutamic acid is denoted as *E1. The amino groups in the side chains of the glutamine and asparagine residues are shown in parentheses, and the *C*-terminal amino group is shown as ($CONH_2$).

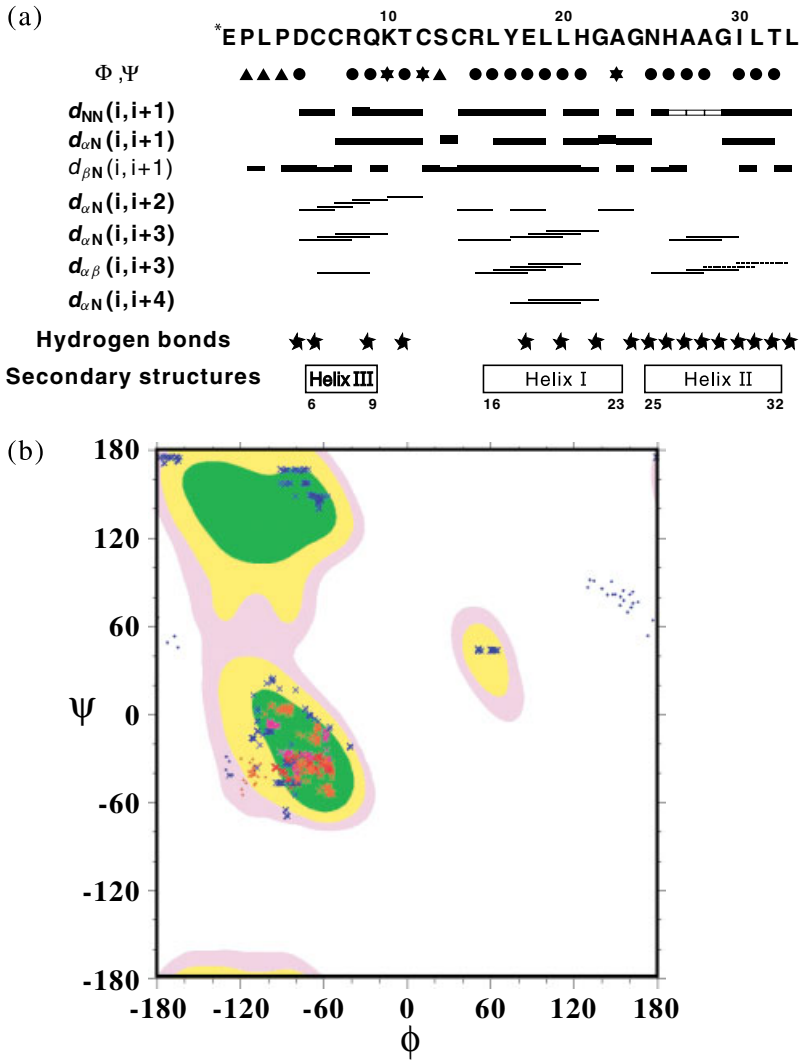

Figure 3 Summary of the structural information obtained from the NMR experiments. (a) The sequential and medium range NOE connectivities are represented by bars, the size of which indicates the NOE intensity (strong, medium, or weak). Amide protons that were exchanged slowly at pH 6.0 and 293 K and assumed to form hydrogen bonds in the structure calculations are indicated. The white bars in $d_{NN(i,i+1)}$ and the dashed bars in $d_{\alpha\beta(i,i+3)}$ represent ambiguous NOE assignments because of the resonance overlaps in the amide protons of Ala27, Ala28, and Gly29 and in the α-protons of Ala28-Leu33, respectively. They were not included as restraints in the structure calculations. The ●, ▲, and ⋆ in ϕ, ψ represent that the combination of the ϕ and ψ dihedral angles for each residue that was predicted by TALOS [19] was within the regions of the Ramachandran plot typical of α-helix ($-175^\circ < \phi < -40^\circ$ and $-90^\circ < \psi < 0^\circ$), β-sheet ($-130^\circ < \phi < -40^\circ$ and $115^\circ < \psi < 180^\circ$ or $-180^\circ < \psi < -150^\circ$), and the region except for the above-mentioned α-helix and β-sheet, respectively. (b) The Ramachandran plot showing distributions of the ϕ and ψ dihedral angles (degree) of residues 1–32. The angles for the glycine residues are plotted by dots. The plots for the residues constituting helices I, II, and III are displayed in orange, red, and magenta, respectively. The figure was produced with MOLMOL [20].

angles of the residues constituting helices I, II, and III are confined within the region characteristic of helices.

Comparison Between the Structures of Orexins-A and -B

Orexin-B dissolved in H_2O consists of two α-helices (helix I: Leu7-Gly19 and helix II: Ala23-Met28) connected with a flexible linker between them (Figure 1(d)), and helix I is oriented 60–80° relative to helix II (Figure 5) [13]. Orexin-A has a compact conformation in the *N*-terminal half region (Pyr1-Arg15) containing a short helix (III: Cys6-Gln9), fixed by the two disulfide bonds, and a helix-turn-helix conformation (I: Leu16-Ala23 and II: Asn25-Thr32) in the remaining *C*-terminal half region. Helices I and II in orexin-A are numbered on the basis of the numbering of the corresponding helices in orexin-B with high sequence homology. The structural features of the *C*-terminal regions of orexins-A and -B are more similar to each other than those of the *N*-terminal regions, reflecting the sequence homology between the two molecules (discussed below in detail).

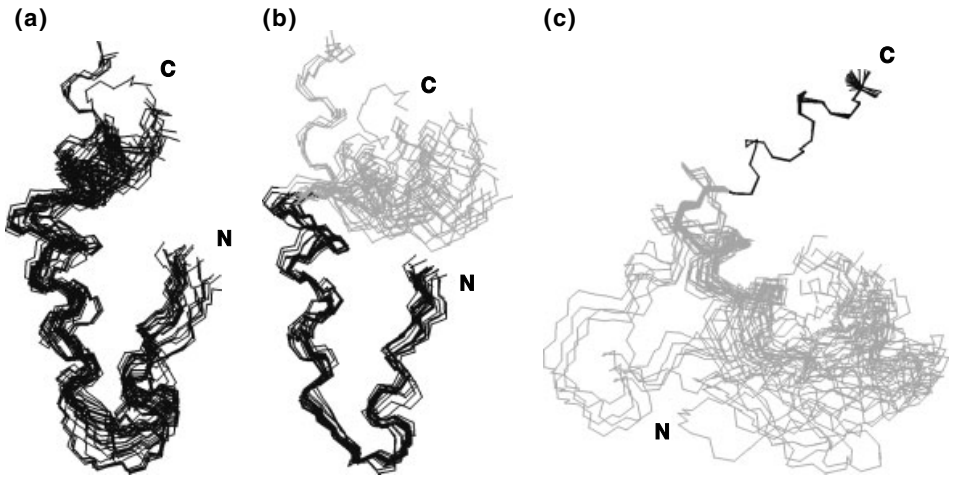

Figure 4 The best-fit superpositioning of the final 30 structures, calculated by means of the simulated annealing procedure of CYANA [18]. The backbone atoms (N, Cα, and C′) in the regions colored black are superimposed. The superimposed ranges and the resultant RMSDs are (a) Pyr1-Leu33, 2.52 Å, (b) Pyr1-Ala23, 0.91 Å, and (c) Asn25-Leu33, 0.34 Å.

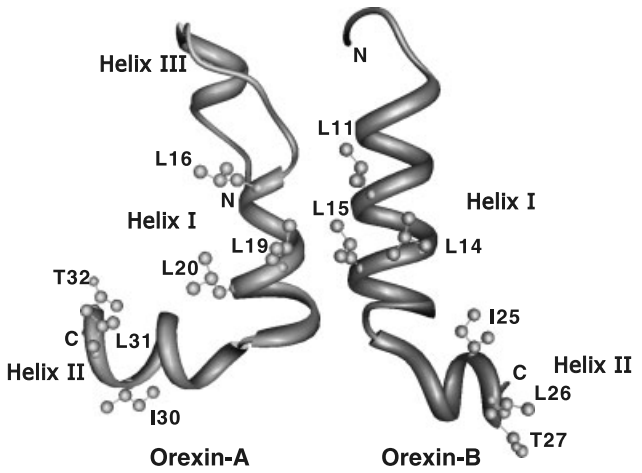

Figure 5 The hydrophobic residues are supposed to be important for the interactions with the receptors. The residues for which the alanine- or proline-scanned experiments both in orexin-A [22] and orexin-B [23] peptides commonly exhibited decreased activities through binding to OX_1R are indicated. The amino acid sequence number (*i*) in orexin-A is aligned to (*i-5*) in orexin-B [13]. The two molecules are arranged so that helices I, including the side chains are aligned in the same orientation.

Comparison with the Structure of Orexin-A in Micelles

The structures of orexin-A bound to SDS micelles, determined by 2D ^{1}H and ^{13}C natural isotopic abundance NMR [11], tend to adopt conformations containing a short helical section (helix III: Asp5-Gln9) and another α-helix (helix I: Leu16-Gly22) connected with a bend (Lys10-Ser13) between them (Figure 1(a)). The ranges of the two helices III and I are almost consistent with our results (Figure 1(a) and (c)). In micelles, the conformation in the region containing helix III and the following bend, and the conformation of helix I, were respectively well converged, but the

Table 1 Structural statistics for the final 30 structures of Orexin-A

Total number of distance restraints	382
Intraresidual	168
Sequential ($\|i-j\|=1$)	119
Medium range ($\|i-j\|\leq 4$)	70
Long range ($\|i-j\|>4$)	16
Hydrogen bonds	9
Number of dihedral angle restrains	48
Maximum violation of distance restraints	0.19 Å
Maximum violation of dihedral angle restraints	4.19°
Maximum violation of *van der Waals* distances	0.15 Å
R.m.s. deviations from experimental restraints	
Distance	0.0079 ± 0.0011 Å
Angle	0.5042 ± 0.1093°
PROCHECK [21] Ramachandran plot statistics (residues1–32)	
Residues in most favored regions	94.6%
Residues in additionally allowed regions	5.4%
Residues in generously allowed regions	0%
Residues in disallowed regions	0%
R.m.s. deviations from mean coordinate positions	
Backbone heavy atoms	
Residues 1–23	0.91 Å
Residues 25–33	0.34 Å
All heavy atoms	
Residues 1–23	1.64 Å
Residues 25–33	1.33 Å

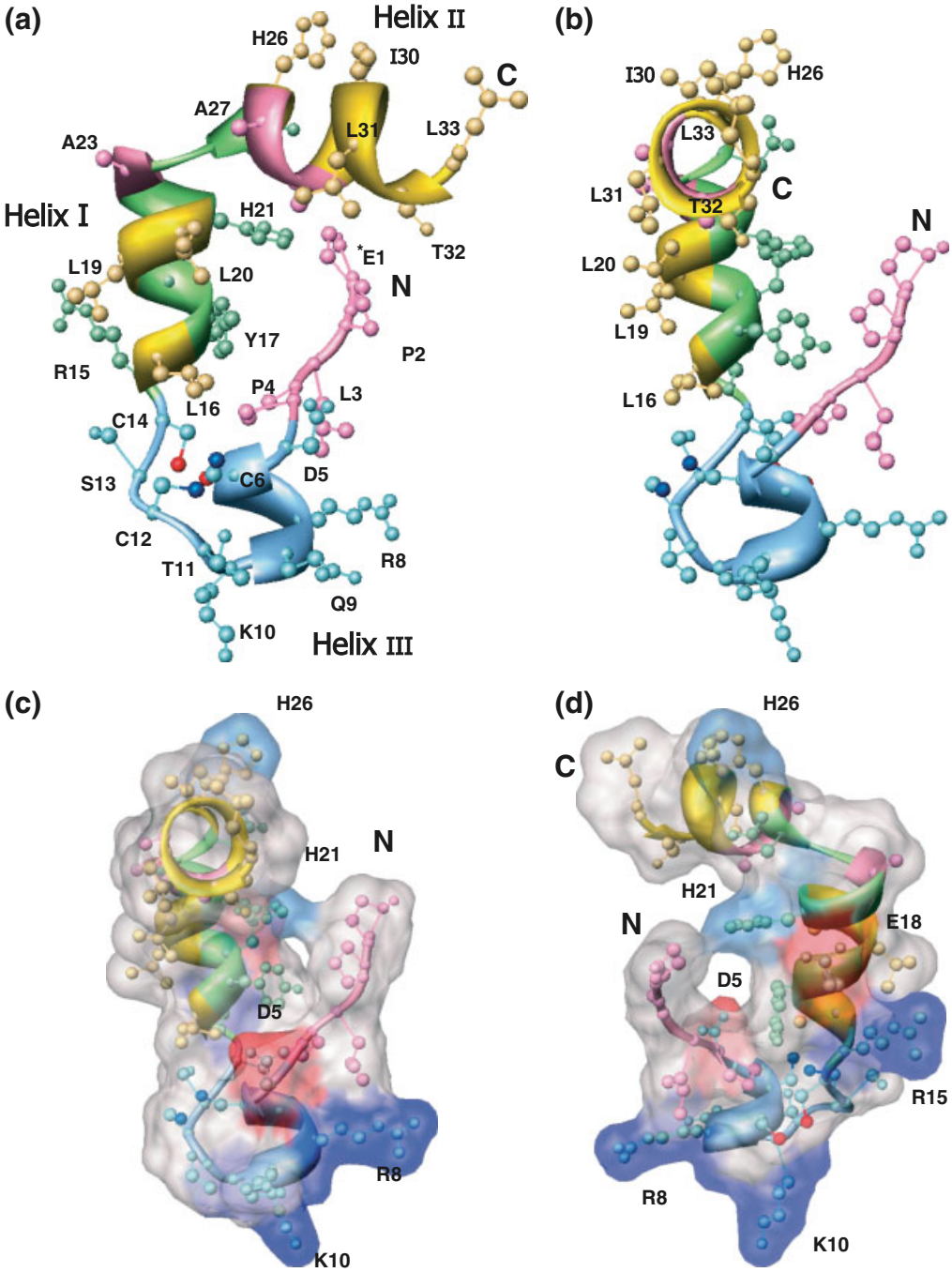

Figure 6 Hydrophobic and hydrophilic surfaces on orexin-A. The residues of which the replacements with alanines in an orexin-A (15–33) truncated peptide resulted in a significant drop in the functional potency at the OX_1R receptor [22] are drawn yellow: Leu16, Leu19, Leu20, His26, Gly29, Ile30, Leu31, Thr32, and Leu33. These residues are almost on one side of orexin-A to form a hydrophobic surface. On the other hand, the residues that contributed to a minor degree to the binding to OX_1R in the alanine-scan experiments [22] are drawn green: Arg15, Tyr17, Glu18, His21, Gly22, Gly24, and Asn25. Hydrophilic and charged residues in the *N*-terminal half region are drawn cyan: Asp5, Arg8, Gln9, Lys10, Thr11, and Ser13. The side chains of the residues drawn green and cyan exist in the direction almost against the hydrophobic patch drawn yellow, forming a rather hydrophilic surface. The molecule (b) is rotated by 55° about the vertical axis with respect to the molecule (a). (c) and (d) The electrostatic potential is mapped on the solvent-accessible surface of orexin-A. Blue corresponds to the positive potential and red to the negative potential. The histidine residues are drawn with a lighter blue, taking their average pKa value of 6.4 into account. The molecule (c) is arranged in the same orientation as (b), and the front of (d) is seen from the backside of (a). The figures were produced with the Chimera program [26].

relative orientation between the two regions and the conformation of the *C*-terminal part (Ala23-Leu33) were not so well defined because of the lack of NOE-based distance information and of spectral overlaps [11]. In any case, orexin-A is likely to prefer having a helical conformation in micelles as well.

DISCUSSION

Separation of Hydrophobic and Hydrophilic Parts in the Structure

Important residues in orexins-A and -B for their binding to the receptors, OX_1R and OX_2R, have so far been extensively analyzed using truncated peptides and alanine-scanned peptides, where each of the natural amino acids were systematically replaced with L-alanine [22–25]. Their activities were estimated from the transient mobilization of the intracellular calcium concentration, which was mediated by the receptors binding with various kinds of synthesized peptides of interest. Darker *et al.* [22] indicated that the substitution of each of the residues, Leu16, Leu19, Leu20, His26, Gly29, Ile30, Leu31, Thr32, and Leu33 with alanine in an orexin-A (15–33) truncated peptide resulted in a significant drop in the functional potency at the OX_1R receptor. In our structures, the side chains of most of these residues exist on one side of orexin-A and form a hydrophobic surface, as displayed in yellow in Figure 6, which may be involved in the interaction with the receptor. Among these residues, Leu16, Leu19, Leu20, Gly29, Ile30, Leu31, and Thr32 correspond, respectively, to Leu11, Leu14, Leu15, Gly24, Ile25, Leu26, and Thr27 in orexin-B (Figure 5), and the latter residues were also shown to be highly involved in the interaction with OX_1R in a similar experiment using alanine- or proline-scanned and truncated orexin-B (6–28) peptides [23]. For the corresponding pairs of these residues in orexins-A and -B, the approximate orientations of the side chains and the kinds of amino acids coincide, indicating that they are commonly important in orexins-A and -B for their interactions, particularly with OX_1R.

On the other hand, most of the residues that showed minor contributions to the binding to OX_1R in the alanine-scan experiments [22], Arg15, Tyr17, Glu18, His21, Gly22, Gly24, and Asn25, place their side chains in a direction almost opposite to the hydrophobic patch, to form a hydrophilic cluster together with the *N*-terminal residues (Asp5-Cys14), as displayed in green and blue in Figure 6. Darker *et al.* [22] described that the charged residues among them, Arg15 and Glu18, played no role at all in the interaction with the receptor, and Ammoun *et al.* [24] also showed that the replacement of Glu18 with alanine in orexin-A (14–33) gave rise to no difference in the interaction with OX_1R compared to the control, and that the replacement of Arg15 led to only a twofold reduction in the potency of the mutated peptide. Interestingly, these residues containing the charged ones, which do not appear to be deeply committed to interaction with the receptor, are found separately from the hydrophobic surface that is likely to interact directly with the receptors (Figure 6). In addition, four of the residues in orexin-A, Tyr17, Glu18, His21, and Gly22, are of different kinds from the sequentially corresponding residues in orexin-B, Gln12, Arg13, Gln16, and Ala17, respectively, which are not largely involved in the interaction with the receptors either [23].

The Function of the *N*-terminal Region

Lang *et al.* [23] suggested that the two disulfide bonds in orexin-A are not required for binding to the receptors, based on the result that both the reduced orexin-A peptides and mutants where the cysteines were replaced with aminobutyric acids (Abu) still maintained almost the same activity as the native orexin-A. Darker *et al.* [22] also indicated that the truncated *C*-terminal orexin-A (15–33) still exhibited a slight 20-fold reduced affinity to OX_1R without losing the complete affinity, compared to the intact orexin-A. In our structures, the hydrophilic and charged residues in the *N*-terminal region cluster, Asp5-Arg15, separated from the hydrophobic surface formed on one side of the *C*-terminal helices I and II (Figure 6). Therefore, the receptors may mainly recognize the hydrophobic *C*-terminal regions of orexins-A and -B, and may not dominantly interact with their *N*-terminal regions.

There are, nevertheless, some significant differences between the *N*-terminal regions of orexins-A and -B. Many of the *N*-terminal residues in orexin-A are hydrophilic ones or ones that tend to be involved in hydrogen bonds in their side chains (Asp5, Arg8, Gln9, Lys10, Thr11, Ser13, and Arg15), forming a rigid conformation suspended further by the two disulfide bonds. On the other hand, the *N*-terminal orexin-B (1-RSGPPGLQG-9), containing no disulfide bond or charged residue except for Arg-1, is composed of a smaller number of residues with almost no sequence homology (11%) to the corresponding part of orexin-A, and the region of 1-RSGPPGL-7 seems to have a loop-like flexible conformation, as can be judged from almost no observable NOE cross peaks [13]. It is known that OX_1R discriminates between orexins-A and -B with more selectivity for orexin-A, and that OX_2R is a nonselective receptor [1]. Thus, the difference in the *N*-terminal regions of orexins-A and -B may be associated with a preference for OX_1R. Some observations have been reported that suggest this idea. The truncated *C*-terminal orexin-A (15–33) and a mutant where Cys6-Cys14 was replaced with Pro-Gly or flexible 6-aminohexanoic acid (Ahx) led to a loss of OX_1R preference [23], and the disulfide bonds

in orexin-A play a key role in OX_1R activation, which may be required for gastric acid secretion [27]. Taking the relationship between these observations and our structure into account, we suggest that the *C*-terminal hydrophobic regions of orexins-A and -B interact with both receptors without a large preference, and that the conformational and electrostatical differences in the *N*-terminal regions of orexins-A and -B are involved in the preference for orexin-A by OX_1R.

Functions of the Pyroglutamate

Orexin-A has a pyroglutamate (2-pyrrolidone-5-carboxylic acid) at the first *N*-terminal residue site, which does not exist in orexin-B. Pyroglutamate has been found at the *N*-terminal ends of a lot of neuropeptides, including thyrotropin-releasing hormone (TRH) [28] and neurotensin [29], and pyroglutamate is thus thought to have important biological and physiological functions [30]. Since pyroglutamate can be chemically made in such a way that the carboxylic group in the side chain of glutamate is cyclized with the amino group of the intraresidue main-chain through dehydration, pyroglutamate no longer has a negative charge at all, but rather possesses a hydrophobic character similar to proline. Lang *et al.* [23] reported that the removal of the first residue from orexin-A led to an OX_1R preferring analogue with 10- and 40-fold decreases in activities at the OX_1R and OX_2R, respectively. In our tertiary structure of orexin-A, the *N*-terminal four hydrophobic residues, including the pyroglutamate (Pyr1-Pro4), protrude from the plane roughly made by the following residues in Asp5-Arg15 and helix I-turn-helix II (Leu16-Leu33) (Figure 6). Thus, the hydrophobic part of the *N*-terminal may interact with another region on the receptors independently of the dominant interaction site involving the *C*-terminal helical region. As an alternative proposal for interpreting the reduction in affinity to the receptors by the removal of the pyroglutamate, the interaction with the receptors might cause a conformational change in orexin-A, especially around Gly-24, which may bring helix II closer to the pyroglutamate to make a wider hydrophobic cluster composed of helices I and II together with the four *N*-terminal residues.

Differences in the *C*-terminal Regions of Orexins-A and -B

Darker *et al.* [22] suggested that the residues from Arg15 to Asn25 in orexin-A play an important conformational role in the interaction with the OX_1R. Lang *et al.* [23] also found the sequence ranging from Arg15 to Leu33 to be the minimal part necessary for activating the receptors. This *C*-terminal half region has the highest sequence homology (68%) with the corresponding region in orexin-B (Arg-10 to Met-28) (Figure 1). Although both regions in orexins-A and -B have helix-loop(turn)-helix conformations, the two helices in orexin-A turn at the position of Gly24, different from the position of the loop in orexin-B (Figures 1 (c) and (d), and 5). In orexin-A, the residue Gly24 plays the role of a hinge, which may cause a fluctuation between helices I and II, as presumed from the resultant dispersed overlay in the overall calculated structures compared to the well-converged overlay in either helix alone (Figure 4). The part in orexin-A (Asn25-His-Ala27) that sequentially corresponds to the loop region in orexin-B (Asn20-His-Ala22) is within helix II. Furthermore, the relative orientations between helices I and II are opposite in orexins-A and -B, although the angle made by them in orexin-A, 81.4° on an average, is almost the same as that in orexin-B. The hydrophobic residues on helices II are, therefore, oriented to the opposite direction in orexins-A and -B when helices I are aligned in the same direction (Figure 5), although the hydrophobic residues are oriented in almost the same direction when either of helices I or II alone are considered. The different conformations of the *C*-terminal orexins-A and -B, both of which were determined in their free forms, might suggest that conformational changes, including shifting of the loop positions and torsion of the helices, occur upon their binding to the receptors.

Preferred Interaction Between Orexin-A and OX_1R

The interactions between each kind of orexins and receptors should also be discussed from the viewpoint of the receptors. Lang *et al.* [23] suggested that the conformations of the side chains of the ligands are more important for the activation of OX_1R with a larger ligand-contact site based on the observation that OX_1R was in general more sensitive to amino acid replacements in orexins than OX_2R. Ammoun *et al.* [24] also obtained similar results. These observations mean that OX_1R has more strict specificity to the orexins than OX_2R. The *C*-terminal parts of orexin-A (Arg15 to Leu33) and orexin-B (Arg10 to Met28) exhibit sequence homology as high as 68%, and have similar conformations basically classified into helix-loop(turn)-helix. However, a detailed structural comparison shows some differences in the lengths of both helices, the positions of the loops, and the relative orientations between the two helices. OX_1R may specifically recognize the differences between the overall conformations, especially the hydrophobic side chains in the *C*-terminal parts of orexins-A and -B with a more exact fit to orexin-A, while OX_2R may recognize them in a more ambiguous way. In addition, we have found clear distinctions between the *N*-terminal parts of the orexins in terms of the conformations and electrostatic characters of the constitutive side chains. Possibly, OX_1R also interacts with the *N*-terminal parts of orexins, although the interaction is not dominant

compared to the recognition of the *C*-terminal part. The weaker association of OX_1R with orexin-B than with orexin-A may be caused by the lack of a recognizable fixed conformation in the *N*-terminal orexin-B, and by the fewer numbers of charge–charge interactions or hydrogen bond formations between the *N*-terminal part of orexin-B and OX_1R.

Asahi *et al.* found that an orexin-B mutant, ([Ala11, D-Leu15]-orexin-B), where Leu11 and Leu15 in the wild type were respectively replaced with L-alanine and D-leucine, showed more selectivity (400-fold) for OX_2R over OX_1R than the wild-type orexin-B, without significant reduction in the potency for the OX_2R. This is probably because the modified helix I region in orexin-B was rejected by OX_1R, whose recognition of the ligands must be stricter than OX_2R, and was, however, still accepted by the more tolerable OX_2R. Although further analyses are required, their result may suggest that the hydrophobic surface of helix I is also possibly involved in the selectivity by the receptors.

Chemical and Conformational Similarity to a Selective OX_1R Antagonist

SB-334 867-A (1-(-2-Methylbenzoxazol-6-yl)-3-[1,5]-naphthyridin-4-yl-urea HCl) is known as a selective OX_1R antagonist [31,32]. When comparing the chemical structure and/or conformation of SB-334 867-A with those of orexin-A, we found that two regions in orexin-A appear to resemble SB-334 867-A. One is the region containing Tyr17 and His21 (Figure 7). Since the two side chains reside on helix I and protrude in the same direction, the two aromatic parts of SB-334 867-A and the ureido part between them can be chemically similar to the side chains of Tyr17 and His21 and to a peptide group between them, respectively. The other similar region in terms of the conformations not of the chemical structures is in the few *N*-terminal residues of orexin-A containing Pyr1 and Pro2 (Figure 7). As described above, the peptide ranging from Arg15 to Leu33 is the minimum part required for binding to OX_1R and activating it [22–24,27], but the remaining *N*-terminal region of orexin-A is likely to be involved in the preference for orexin-A of OX_1R, as observed by the loss of preference caused by the deletion of Pyr1-Ser13 (Cys14) [23]. The fact that SB-334 867-A binds to OX_1R with a 50-fold selectivity over OX_2R [31] might suggest that SB-334 867-A mimics the *N*-terminal region of orexin-A, which does not exist in orexin-B, rather than the *C*-terminal region containing helix I. The *C*-terminal region of orexin-A is important not only for binding to the receptor but also for activating it. If SB-334 867-A binds to the same surface on OX_1R as the Pyr1-Pro2 part of orexin-A does, the function of SB-334 867-A as an antagonist, without activating the receptor [32], could be explained by the lack of a chemical structure corresponding to the *C*-terminal region of orexin-A.

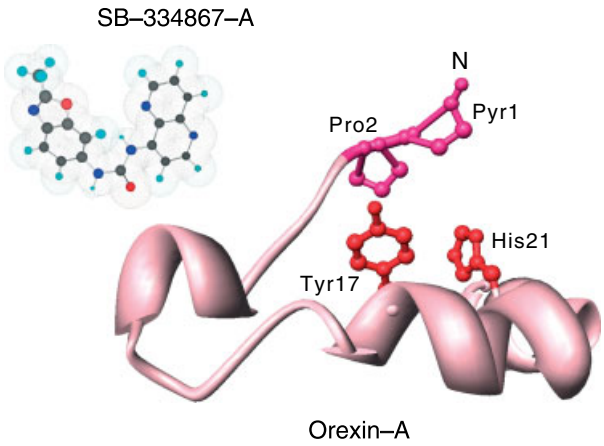

Figure 7 Comparison between a selective OX_1R antagonist, SB-334 867-A, and orexin-A. Two regions in orexin-A that appear structurally or chemically similar to the antagonist are shown red in a ball-and-stick model. The region containing Tyr17 and His21 may resemble the antagonist in terms of its chemical structure and conformation. In particular, the orientations of the two aromatic rings in orexin-A and the antagonist are similar to each other. The other region containing Pyr1 and Pro2 is not similar chemically to the antagonist, but the conformation appears similar to that of the antagonist. The chemical structure of SB-334 867-A was at first drawn using ChemDraw (CambridgeSoft). Then, its conformation was subjected to a molecular dynamics simulation (MM2) in Chem3D (CambridgeSoft), and the energy was finally minimized by the semiempirical PM3 method, a kind of quantum mechanical method, using the MOPAC program and default parameters in Chem3D. Each sphere in the ball-and-stick model represents hydrogen (cyan), carbon (grey), nitrogen (blue), and oxygen (red). The dot surfaces represent the *van der Waals* radii of the constituting atoms.

Possible Conformational Exchange in the *N*-terminal Region

Another structure of orexin-A determined by NMR was presented very recently by Kim *et al.* [12]. Their structure was similar to our structure in the *C*-terminal regions composed of the two α-helices (Figure 1(b) and (c)), while their conformations in the *N*-terminal part were not so well defined and were dispersed when the coordinates of the *C*-terminal regions were overlaid, being significantly different from ours. Detailed analysis, although conducted with difficulty, allowed us to extract a high enough number of NOE-based distance restraints to define the conformation in the *N*-terminal region. When we applied the distance and dihedral angle restraints used for our calculation to their structure (PDB:1R02), we found that 5 of the 6 violations for the distance restraints, and 14 of the 23 violations for the dihedral angle restraints, most of which were over 100°, existed within the *N*-terminal half region. The remaining distance violation (7 Å) between His21 and Asn25 was related to the bending between helices I and II. Since we measured the NMR spectra

of orexin-A dissolved in D_2O to suppress the radiation damping and residual large water signal at 20 °C using an 800 MHz NMR machine equipped with a cryogenic probe, we may have been able to observe otherwise impossible small NOE peaks to refine the structure.

Nevertheless, Kim *et al.* [12] also discussed the importance of the *N*-terminal turn region, including the two disulfide bonds; it may interact with OX_1R and play a role for OX_1R in exhibiting selectivity for orexin-A. Here, we propose a possible conformational exchange that may be occurring in the *N*-terminal region and discuss its biological meaning in binding to the receptors by comparing their structure and ours as well as the conformation of orexin-A in micelles [11]. We particularly have an interest in the circular dichroism (CD) spectroscopic results reported by Kim *et al.* [12], which showed an increase in the helicity of orexin-A in a membrane mimetic condition (DPC-micelle). Some other hormone peptides are also known to have flexible unspecified conformations in solution and to form helix-rich conformations upon interacting with membranes or being embedded in micelles [33]. Furthermore, the conformations of such hormone peptides on membranes or in micelles are often similar to the conformations that are formed upon interaction with the related receptors. Similarly, in orexin-A, its *N*-terminal region in particular, may have a rather flexible conformation in the free state under the equilibrium of exchanging with a helix-containing conformation to be adopted on membranes. Following the interaction with membranes, the equilibrium may completely shift to a more helix-containing conformation such as the one we determined, which may be closer to the yet unknown conformation in the receptor-bound state. This model could explain the following results: (i) The lower sensitivity of the NOE cross peaks associated with the *N*-terminal region may be due to the possible equilibrium between the flexible and helix-containing conformations in the free state. (ii) Thus, the structure of Kim *et al.* [12] may be close to the former one and our structure to the latter. (iii) Orexin-A in SDS micellar solution actually exhibited, although with a low quality, clear helix-like conformation in the *N*-terminal region (Figure 1(a)) [11]) as was also consistent with the CD experimental results [12]. The real structural mechanism of orexin-A and its association with the receptors would be elucidated by the higher quality structures of orexin-A interacting with (bound to) micelles or receptors, for which we are currently investigating.

Acknowledgements

This work was supported by a research grant from the Protein-3000 project from the Ministry of Education, Culture, Sports, Science, and Technology of Japan. The authors thank Ms Naoko Matsuda, Ms Hitomi Kanda, Ms Eriko Chikaishi, Mr Yasushi Kondo, Dr Mamoru Tanida, and Dr Guy T. Hanke for helpful discussions.

REFERENCES

1. Sakurai T, Amemiya A, Ishii M, Matsuzaki I, Chemelli RM, Tanaka H, Williams SC, Richardson JA, Kozlowski GP, Wilson S, Arch JR, Buckingham RE, Haynes AC, Carr SA, Annan RS, McNulty DE, Liu WS, Terrett JA, Elshourbagy NA, Bergsma DJ, Yanagisawa M. Orexins and orexin receptors: a family of hypothalamic neuropeptides and G protein-coupled receptors that regulate feeding behavior. *Cell* 1998; **92**: 573–585.
2. De Lecea L, Kilduff TS, Peyron C, Gao X, Foye PE, Danielson PE, Fukuhara C, Battenberg EL, Gautvik VT, Bartlett FS II, Frankel WN, Van den Pol AN, Bloom FE, Gautvik KM, Sutcliffe JG. The hypocretins: hypothalamus-specific peptides with neuroexcitatory activity. *Proc. Natl Acad. Sci. U.S.A.* 1998; **95**: 322–327.
3. Chemelli RM, Willie JT, Sinton CM, Elmquist JK, Scammell T, Lee C, Richardson JA, Williams SC, Xiong Y, Kisanuki Y, Fitch TE, Nakazato M, Hammer RE, Saper CB, Yanagisawa M. Narcolepsy in orexin knockout mice: molecular genetics of sleep regulation. *Cell* 1999; **98**: 437–451.
4. Date Y, Ueta Y, Yamashita H, Yamaguchi H, Matsukura S, Kangawa K, Sakurai T, Yanagisawa M, Nakazato M. Orexins, orexigenic hypothalamic peptides, interact with autonomic, neuroendocrine and neuroregulatory systems. *Proc. Natl Acad. Sci. U.S.A.* 1999; **96**: 748–753.
5. Hungs M, Mignot E. Hypocretin/orexin, sleep and narcolepsy. *BioEssays* 2001; **23**: 397–408.
6. Sakurai T. Roles of orexins in the regulation of feeding and arousal. *Sleep Med.* 2002; **3**: S3–S9.
7. Volkoff H, Bjorklund JM, Peter RE. Stimulation of feeding behavior and food consumption in the goldfish, Carassius auratus, by orexin-A and orexin-B. *Brain Res.* 1999; **846**: 204–209.
8. Rodgers RJ, Ishii Y, Halford JC, Blundell JE. Orexins and appetite regulation. *Neuropeptides* 2002; **36**: 303–325.
9. Beck B, Richy S. Hypothalamic hypocretin/orexin and neuropeptide Y: divergent interaction with energy depletion and leptin. *Biochem. Biophys. Res. Commun.* 1999; **258**: 119–122.
10. Lopez M, Seoane L, Garcia MC, Lago F, Casanueva FF, Senaris R, Dieguez C. Leptin regulation of prepro-orexin and orexin receptor mRNA levels in the hypothalamus. *Biochem. Biophys. Res. Commun.* 2000; **269**: 41–45.
11. Miskolzie M, Kotovych G. The NMR-derived conformation of orexin-A: an orphan G-protein coupled receptor agonist involved in appetite regulation and sleep. *Biomol. Struct. Dyn.* 2003; **21**: 201–210.
12. Kim HY, Hong E, Kim JI, Lee W. Solution structure of human orexin-A: regulator of appetite and wakefulness. *J. Biochem. Mol. Biol.* 2004; **30**: 565–573.
13. Lee J, Bang E, Chae K, Kim J, Lee D, Lee W. Solution structure of a new hypothalamic neuropeptide, human hypocretin-2/orexin-B. *Eur. J. Biochem.* 1999; **266**: 831–839.
14. Voisin T, Rouet-Benzineb P, Reuter N, Laburthe M. Orexins and their receptors: structural aspects and role in peripheral tissues. *Cell. Mol. Life Sci.* 2003; **60**: 72–87.
15. Cavanagh J, Fairbrother WJ, Palmer AG III, Skelton NJ. *Protein NMR Spectroscopy*. Academic Press: San Diego, 1996.
16. Delaglio F, Grzesiek S, Vuister GW, Zhu G, Pfeifer J, Bax A. NMRPipe: a multidimensional spectral processing system based on UNIX pipes. *J. Biomol. NMR* 1995; **6**: 277–293.
17. Wüthrich K. *NMR of Proteins and Nucleic Acids*. John Wiley & Sons: New York, 1986.
18. Guntert P, Mumenthaler C, Wuethrich K. Torsion angle dynamics for NMR structure calculation with the new program DYANA. *J. Mol. Biol.* 1997; **273**: 283–298.
19. Cornilescu G, Delaglio F, Bax A. Protein backbone angle restraints from searching a database for chemical shift and sequence homology. *J. Biomol. NMR* 1999; **13**: 289–302.
20. Koradi R, Billeter M, Wuthrich K. MOLMOL: a program for display and analysis of macromolecular structures. *J. Mol. Graph.* 1996; **14**: 51–55.

21. Laskowski RA, Rullmannn JA, MacArthur MW, Kaptein R, Thornton JM. AQUA and PROCHECK-NMR: programs for checking the quality of protein structures solved by NMR. *J. Biomol. NMR* 1996; **8**: 477–486.
22. Darker JG, Porter RA, Eggleston DS, Smart D, Brough SJ, Sabido-David C, Jerman JC. Structure-activity analysis of truncated orexin-A analogues at the orexin-1 receptor. *Bioorg. Med. Chem. Lett.* 2001; **11**: 737–740.
23. Lang M, Soll RM, Durrenberger F, Dautzenberg FM, Beck-Sickinger AG. Structure-activity studies of orexin A and orexin B at the human orexin 1 and orexin 2 receptors led to orexin 2 receptor selective and orexin 1 receptor preferring ligands. *J. Med. Chem.* 2004; **47**: 1153–1160.
24. Ammoun S, Holmqvist T, Shariatmadari R, Oonk HB, Detheux M, Parmentier M, Akerman KE, Kukkonen JP. Distinct recognition of OX1 and OX2 receptors by orexin peptides. *J. Pharmacol. Exp. Ther.* 2003; **305**: 507–514.
25. Asahi S, Egashira S, Matsuda M, Iwaasa H, Kanatani A, Ohkubo M, Ihara M, Morishima H. Development of an orexin-2 receptor selective agonist, [Ala(11), D-Leu(15)] orexin-B. *Bioorg. Med. Chem. Lett.* 2003; **13**: 111–113.
26. Pettersen EF, Goddard TD, Huang CC, Couch GS, Greenblatt DM, Meng EC, Ferrin TE. UCSF Chimera – A visualization system for exploratory research and analysis. *J. Comput. Chem.* 2004; **25**: 1605–1612.
27. Okumura T, Takeuchi S, Motomura W, Yamada H, Egashira S, Asahi S, Kanatani A, Ihara M, Kohgo Y. Requirement of intact disulfide bonds in orexin-A-induced stimulation of gastric acid secretion that is mediated by OX1 receptor activation. *Biochem. Biophys. Res. Commun.* 2001; **2**: 976–981.
28. Boler J, Enzmann F, Folkers K, Bowers CY, Schally AV. The identity of chemical and hormonal properties of the thyrotropin releasing hormone and pyroglutamyl-histidyl-proline amide. *Biochem. Biophys. Res. Commun.* 1969; **37**: 705–710.
29. Carraway R, Leeman SE. The amino acid sequence of a hypothalamic peptide, neurotensin. *J. Biol. Chem.* 1975; **10**: 1907–1911.
30. Awade AC, Cleuziat P, Gonzales T, Robert-Baudouy J. Pyrrolidone carboxyl peptidase (Pcp): an enzyme that removes pyroglutamic acid (pGlu) from pGlu-peptides and pGlu-proteins. *Proteins* 1994; **20**: 34–51.
31. Duxon MS, Stretton J, Starr K, Jones DN, Holland V, Riley G, Jerman J, Brough S, Smart D, Johns A, Chan W, Porter RA, Upton N. Evidence that orexin-A-evoked grooming in the rat is mediated by orexin-1 (OX1) receptors, with downstream 5-HT2C receptor involvement. *Psychopharmacology* 2001; **1**: 203–209.
32. Smart D, Sabido-David C, Brough SJ, Jewitt F, Johns A, Porter RA, Jerman JC. SB-334 867-A: the first selective orexin-1 receptor antagonist. *Br. J. Pharmacol.* 2001; **132**: 1179–1182.
33. Inooka H, Ohtaki T, Kitahara O, Ikegami T, Endo S, Kitada C, Ogi K, Onda H, Fujino M, Shirakawa M. Conformation of a peptide ligand bound to its G-protein coupled receptor. *Nat. Struct. Biol.* 2001; **8**: 161–165.

